Chapter 10

Nutrient Cycling and Tropical Soils

PLATE 10-1

A fallen leaf in a tropical humid forest undergoes a complex process of decomposition involving multiple organisms as the minerals contained in the leaf are eventually released back into the abiotic pool, where they are again taken up by plants.

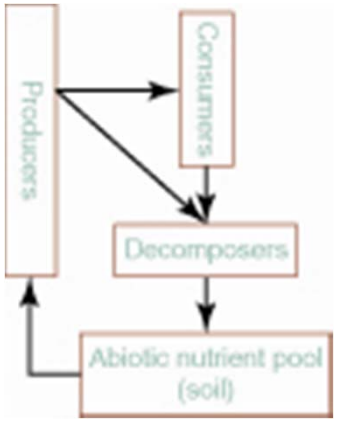

FIGURE 10–1

Simplified compartment model showing the recycling system of an ecosystem such as a tropical forest. Compartments are not to scale. Note that decomposers ultimately make mineral nutrients such as phosphorus available again to primary producers, which take them up during the process of photosynthesis. See text for details.

PLATE 10-2

The Amazon River at midday at a wide point. Notice how the clouds have formed over the forest but not over the river. The clouds reflect the transpiration process vital to the physiology of the forest trees.

PLATE 10-3

This array of tropical leaves demonstrates the waxy quality that they typically exhibit, as well as drip-tips.

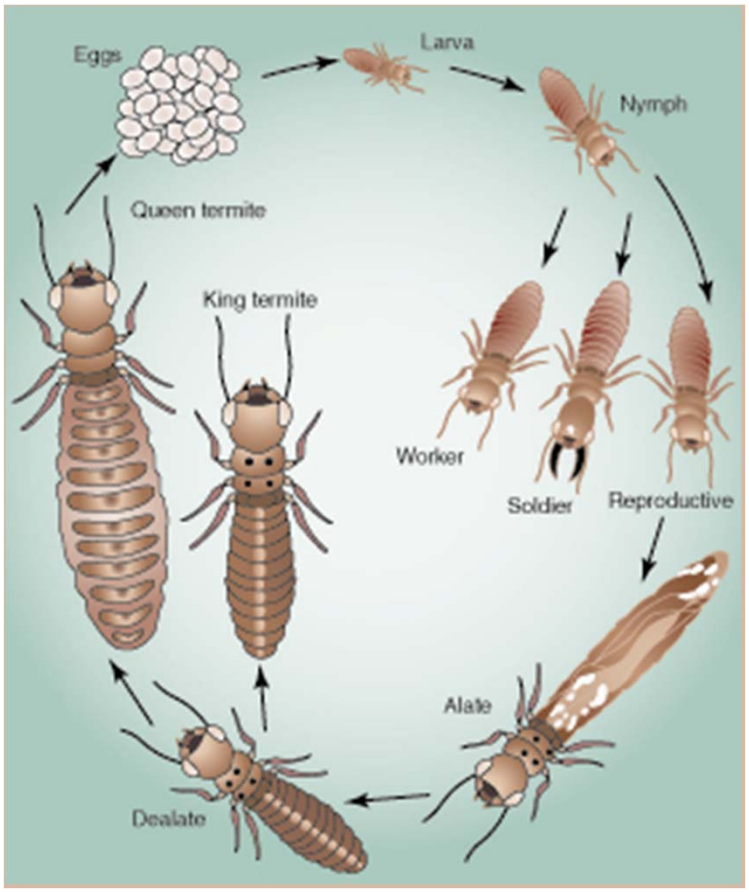

FIGURE 10–2

Termites are abundant throughout the tropics and have an immense influence on nutrient cycling. They also have a complex life cycle in which all reproduction is done by a queen termite.

(a)

(b)

PLATE 10-4

(a) Basketball-size termite mounds such as this are common sights throughout much of the Neotropics. (b) This termite nest has been cut open and is swarming with worker termites repairing the damaged nest.

PLATE 10-5

Look closely among the yellow flowering plants and see the large number of conical termite mounds in this dry forest area in southern Brazil.

(a)

(b)

PLATE 10-6

(a) Large termite mounds such as this are common throughout much of the Australian outback. The nearby trees likely bene3 t in nutrient uptake from proximity to the termite colony. (b) The author (third from left) and three colleagues are dwarfed by the size of the termite “skyscraper” typical of termite mounds throughout much of the Australian outback.

PLATE 10-7

This ball of spines is a sleeping echidna. Eight species of echidna are found in Australia. They are *monotremes*, egg-laying mammals, and they all have a fondness for devouring termites and ants.

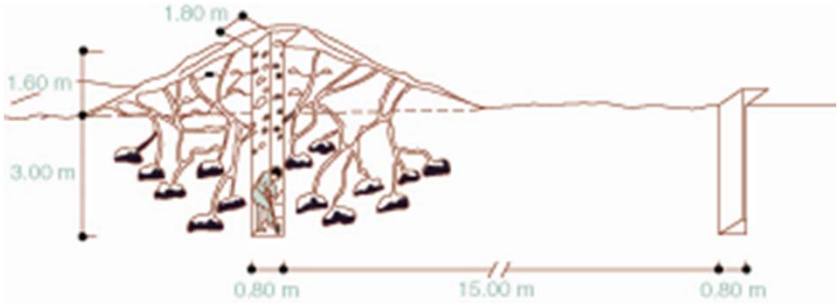

FIGURE 10–3

This is a diagram illustrating the methodology employed in excavation of shafts in the nests of *Atta* ants. Chambers with black dots are refuse chambers, and the others are fungus chambers. Note the overall size of the colony relative to the human figure.

PLATE 10-8

These trees are presumably bene3 ting from growing directly out of an *Atta* nest.



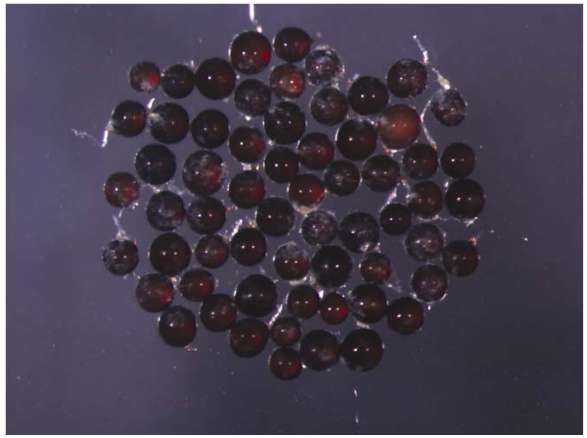


PLATE 10-9

These are images of spores from four species of mycorrhizal fungi.

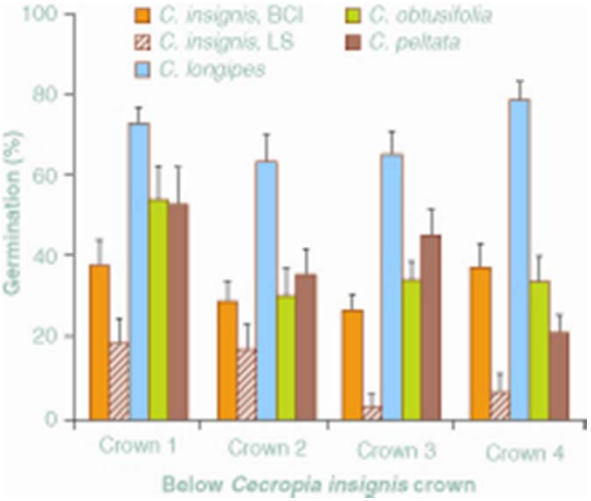

FIGURE 10–4

Differences in seed germination among *Cecropia* species at sites below four crowns of *C. insignis* trees at Barro Colorado Nature Monument, Panama. Bars represent the mean percentage (+SE) of germination success of 20 samples from each species at a given site. Abbreviations are: BCI, Barro Colorado Island; LS, La Selva.

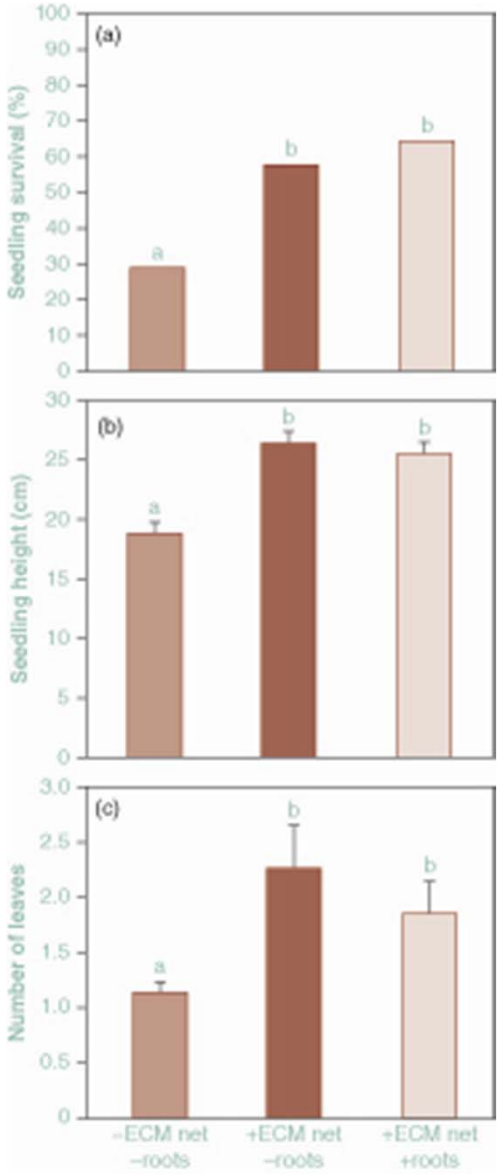

FIGURE 10–5

(a) Survival, (b) height, and (c) number of leaves across treatments for *Dicymbe corymbosa* seedlings after one year. Light brown bars (far left) represent the fine mesh net treatment where common ECM net access and root passage were restricted. Dark brown bars (center) represent the coarse mesh treatment where access to the common ECM net was permitted but root passage was restricted. Tan bars (far right) represent control treatments (no mesh) where ECM net and root passage were both permitted. Bars with different letters indicate significant differences between means of seedlings across treatments (P , /= 0.05). Each treatment was replicated 16 times for a total of 48 experimental units.

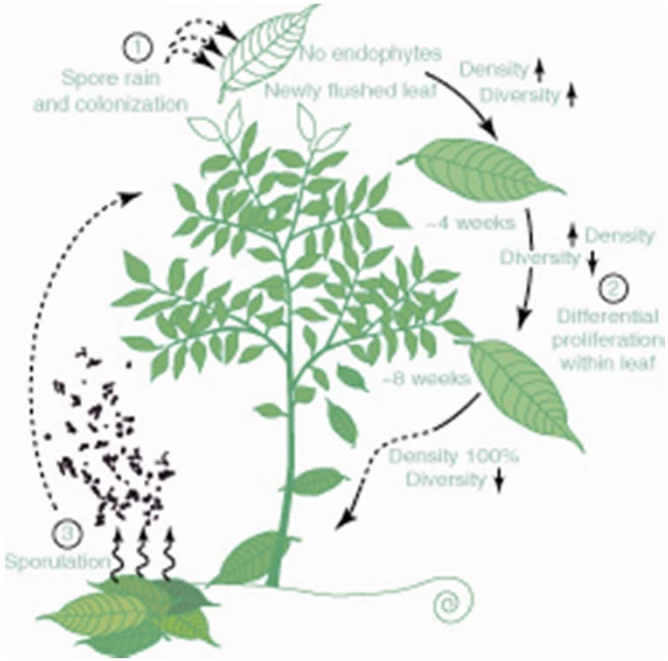

FIGURE 10–6

Proposed life cycle for tropical foliar endophytic fungi (FEF) and their host plants. Leaves are flushed, essentially free of FEF; spores land on the leaf surfaces and, upon wetting, germinate and penetrate the leaf cuticle. After a few weeks, the density of FEF infection within the leaf appears to saturate with a very high FEF diversity. Over several months, FEF diversity usually declines. After leaf senescence and abscission, FEF sporulate, and the cycle begins anew.

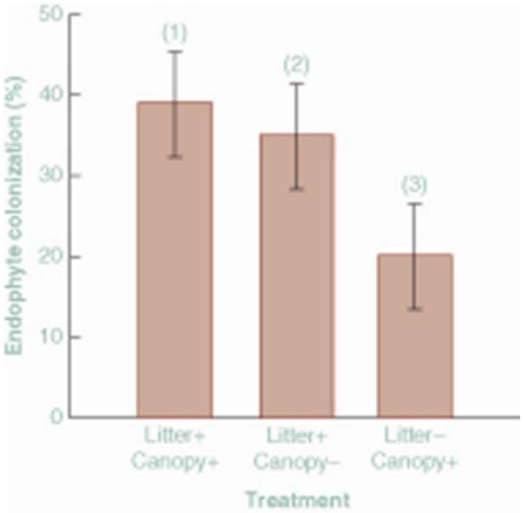

FIGURE 10–7

Local leaf litter is a more important source of foliar endophytic fungal inoculum than intact canopy cover. Mean percentage (±SE) of leaf tissue colonized by endophytes in endophyte-free seedlings of *Theobroma cacao* after a one-week exposure to each of three habitats: (1) intact forest (closed canopy with intact litter, + +; *n* = 15); (2) forest gap (open canopy but with leaf litter intact, - +; *n* = 16); (3) intact forest (closed canopy, with ~90% leaf litter removed within > 20 meters of the seedlings, + -; *n* = 16). One leaf from each seedling was sampled, with 64 2-millimeter-square fragments per leaf assayed for endophyte infection.

(a)

(b)

(c)

PLATE 10–10

(a) to (c) Three examples of the fruiting (spore-producing) bodies of the many kinds of fungi found in Neotropical forests. (c) Note the 3 ies on and around the stinkhorn mushroom (*Dictyphora*). It emits an odor that attracts them, and they aid in dispersing spores.

PLATE 10–11

Leaf litter is abundant in tropical moist forests, but decomposition is sufficiently rapid that in many areas the litter layer is relatively thin.

PLATE 10–12

The species of leaf as well as the overall quality of leaf litter, such as available phosphorus, are important in determining how rapidly the leaf will be decomposed.

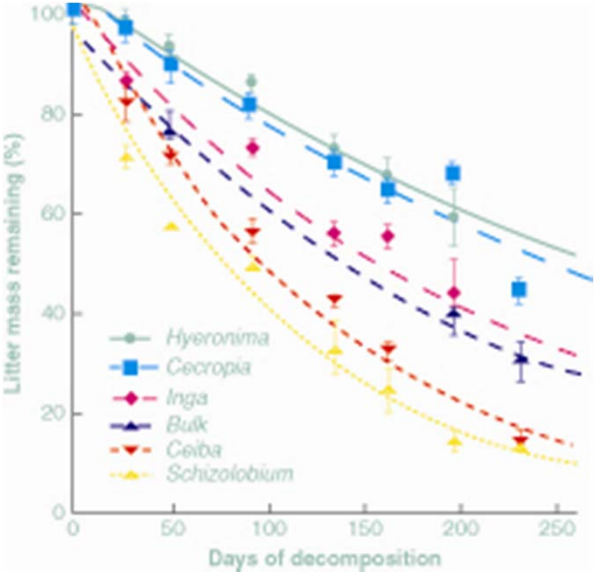

FIGURE 10–8

Decomposition curves illustrating how different genera of trees have different rates of decomposition. All trees were on control plots. Points are means ± standard error and are significantly different from one another.

PLATE 10–13

Red Oxisols such as are revealed in this roadcut in Belize are common throughout much of the tropics.

PLATE 10-14

This farm along the Amazon River is sustained by the rich soil (ultimately from the Andes Mountains) that is annually renewed in the flooding cycle. Note the grove of bananas.

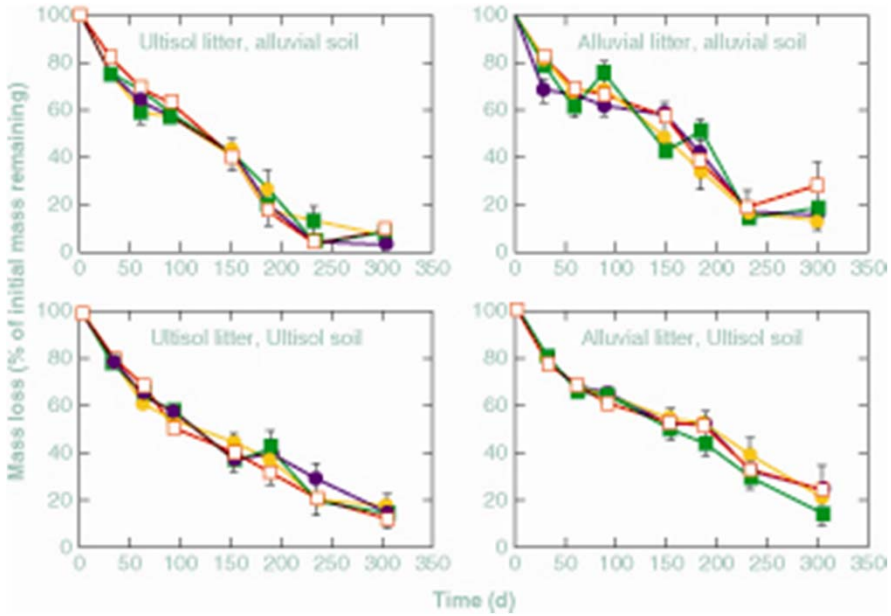

FIGURE 10–9

Effects of nutrient fertilization on loss of organic matter mass shown as percentage of mass remaining (mean ±SE). Treatment types are represented by purple circles (control), yellow circles (N added), solid squares (P added), and open squares (N + P added).

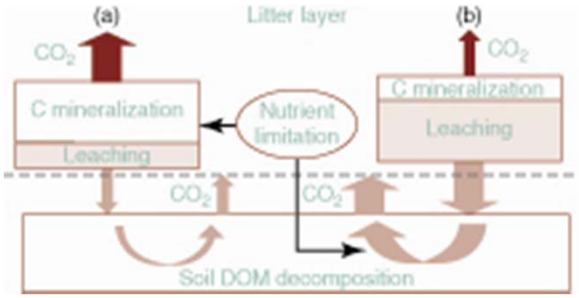

FIGURE 10-10

Conceptual model of the effects of nutrients on decomposition in systems where mass loss from the litter layer is dominated by (a) C mineralization or (b) leaching losses of dissolved organic matter (DOM) to the soil. Nutrient availability may constrain mass loss directly if most C mineralization occurs in the litter layer (a). However, in systems with high precipitation and/or highly water-soluble litter, nutrient availability may not limit mass loss (b) but may ultimately regulate DOM mineralization in the soil. The size (dark of the solid arrows represents the relative flux of either CO2 brown arrows) or leached DOM (light brown arrows).

PLATE 10–15

The nodules on the roots contain the symbiotic bacteria that facilitate uptake of nitrogen.

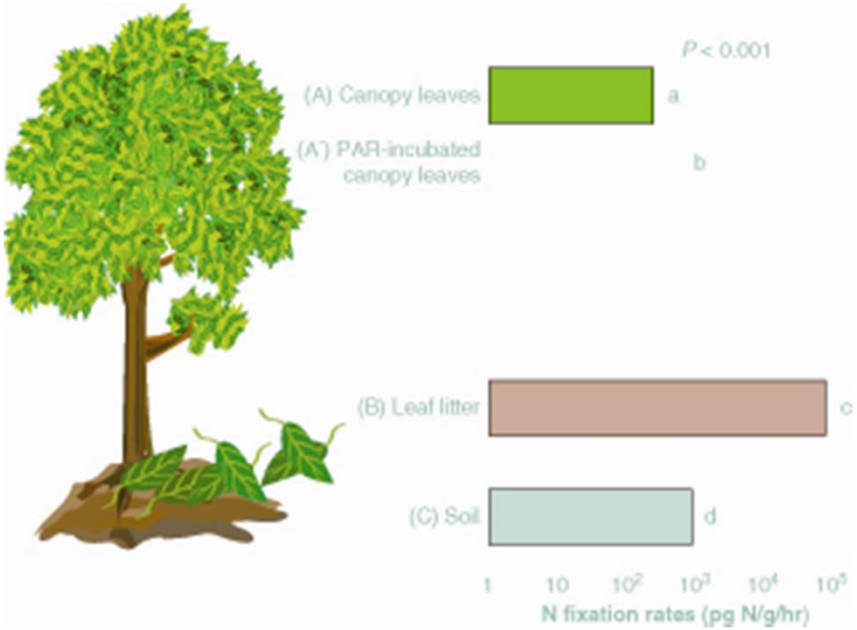

FIGURE 10–11

Rates of free-living N fixation along a rain forest vertical profile: (A) sunlit canopy leaves, (A') sunlit canopy leaves incubated under elevated photosynthetically active radiation (PAR), (B) mixed-species leaf litter, and (C) topsoil (0 to 2 cm). Nitrogen fixation rates (pg/g/hr) varied along the vertical profile (P <.001), and means ($n \approx 48$ trees per layer) $\pm$SE are presented on a logarithmic scale (x axis). Significant differences ($P < 0.05$) in N fixation rates among groups are denoted by different lowercase letters.

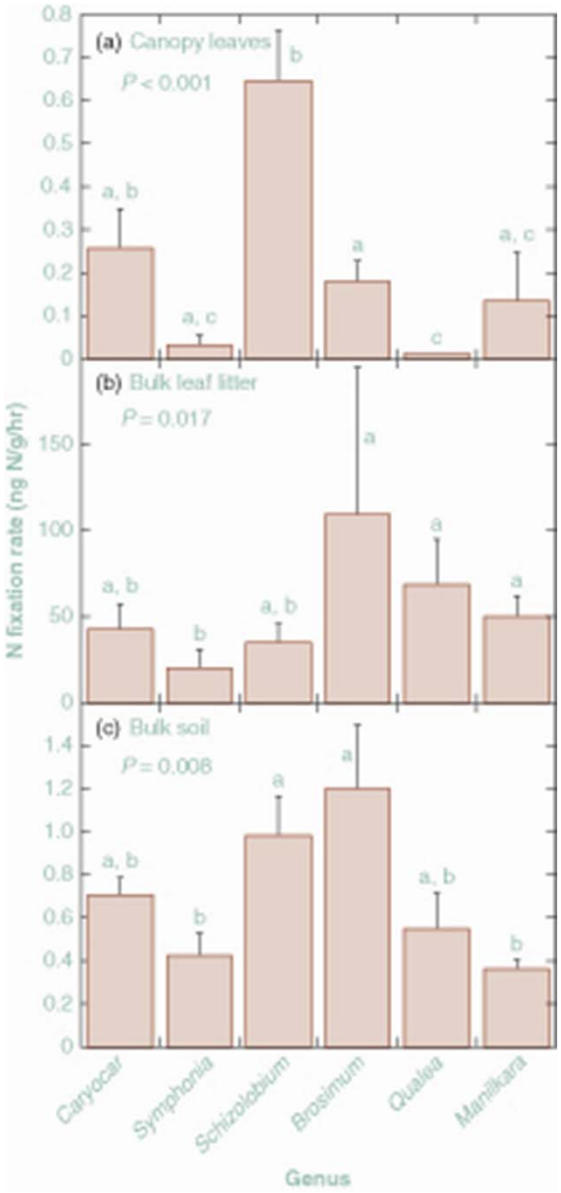

FIGURE 10–12

Comparisons of free-living N fixation rates among six tree species incubated on the forest floor for (a) sunlit canopy leaves, (b) mixed-species bulk leaf litter, and (c) surface soil (0 to 2 cm) collected within the crown radius of trees. Free-living N fixation rates were significantly different among the six tree species within each forest component ($P < 0.05$ for each), and significant differences among species within a component are denoted by different lowercase letters. N fixation rates (ng/g/hr) are means ($n \geq 7$ trees per species for each layer) ±SE. Note that the *y*-axis scale is different for each component.

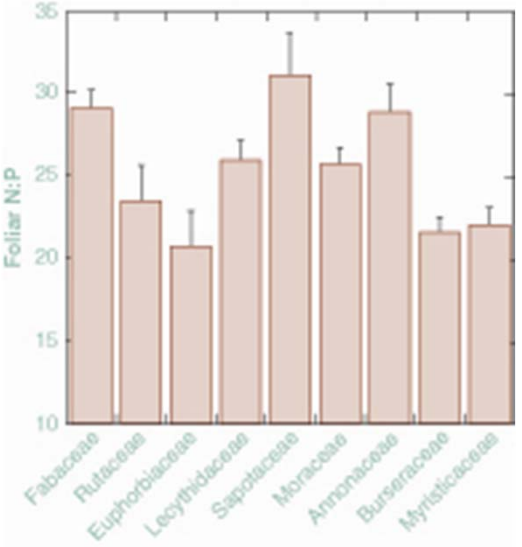

FIGURE 10–13

Variation in N : P among various plant families.

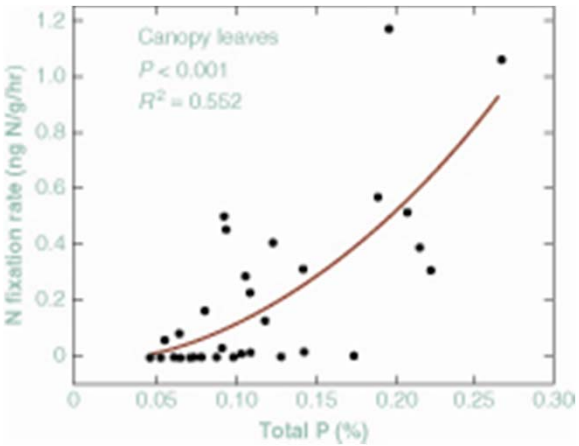

FIGURE 10–14

Total phosphorus as a function of nitrogen fixation rate for canopy leaves.

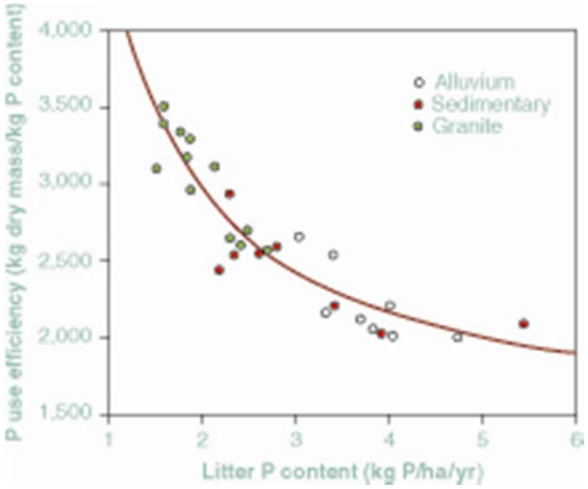

FIGURE 10–15

The P use efficiency of litter production along a P gradient in lowland rain forest at Gunung Palung National Park, Indonesia.

PLATE 10-16

Thick deposits of sediment characterize this section of the Napo River in Ecuador. Such sediment is rich in nutrients.

PLATE 10-17

This photo shows sediment deposit on an island along the Amazon River approaching Manaus, Brazil. The river deposits sediment but also sweeps it away, depending on the flood cycle. This creates dynamic islands within the river.

PLATE 10–18

The “wedding of the waters,” when the dark, mocha-colored, sediment-rich Amazon intersects with the clear, dark, sediment-poor Rio Negro. This confluence occurs near Manaus, Brazil.

PLATE 10–19

Parrots of several species at a *collpa* along the Napo River in Ecuador.

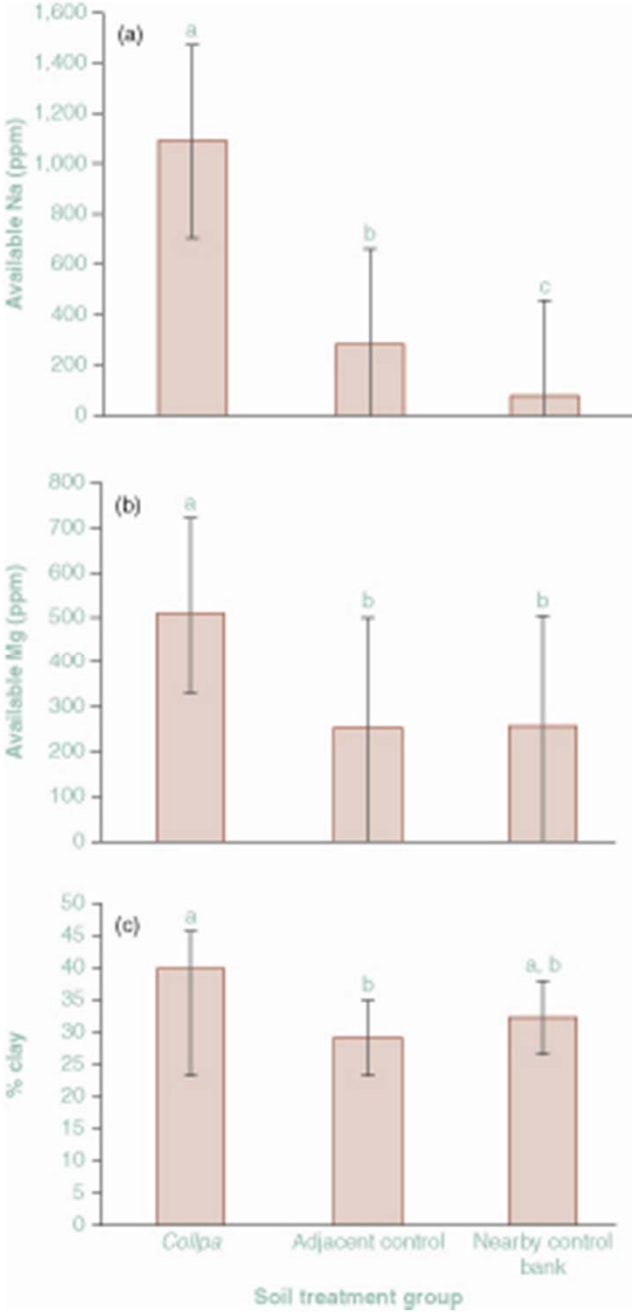

FIGURE 10–16

(a) Mean available sodium concentration, (b) mean available magnesium concentration, and (c) percent clay of soils in three treatments: *collpa,* adjacent controls, and nearby control banks (n = 18 for each). Error bars represent mean ±95% CI calculated using error terms in the ANOVA models. Treatment groups with the same lowercase letter indicate that rank-transformed values were not significantly different (α = 0.05). Treatment group comparisons shown for percent clay despite marginal overall model significance (P = 0.075).

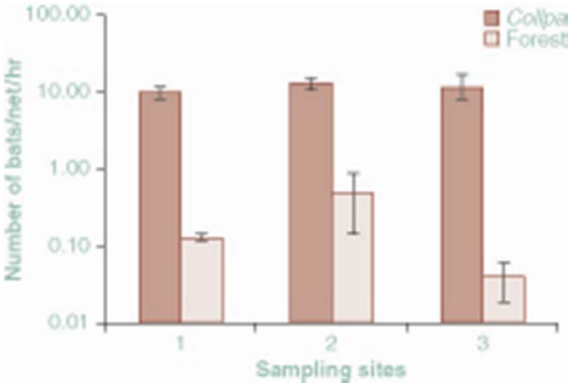

FIGURE 10–17

Bat captures (number of bats/net/hour) ±SE for collpas and non-collpa forest sites in southeast Peru.

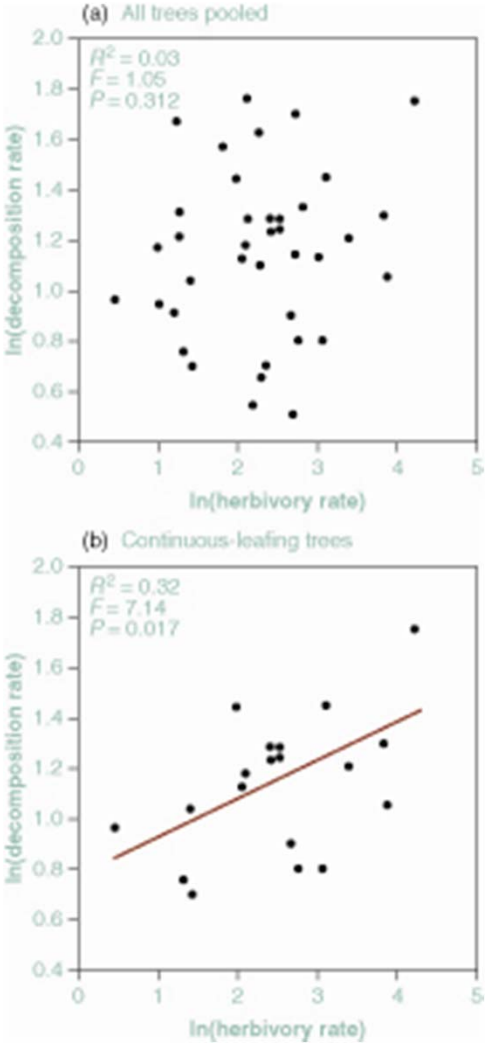

FIGURE 10–18

Comparison between all trees pooled (a) and continuous-leafing trees (b) with regard to the relationship between leaf decomposition rate and herbivory rate. Only continuously-leafing trees showed a strong correlation between the variables.

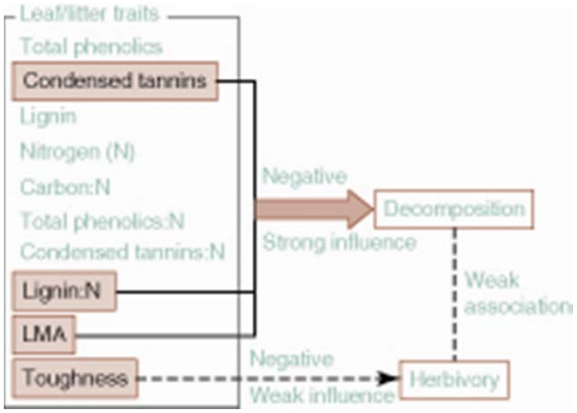

FIGURE 10–19

Relationships between herbivory and decomposition rates across tree species, and leaf and litter traits related to these rates in a Malaysian tropical rain forest. Solid, wide arrows indicate a strong influence, dashed arrows indicate a weak influence, and dashed lines indicate a weak association.

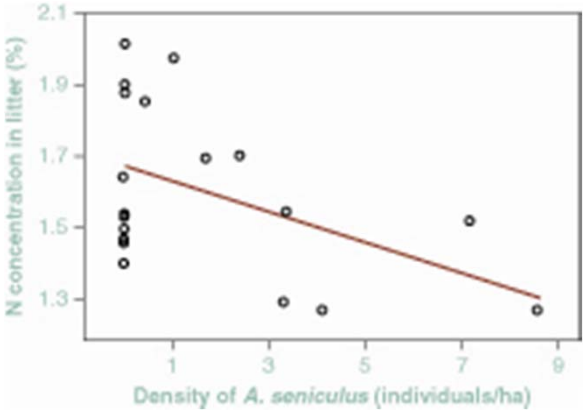

FIGURE 10–20

The concentration of nitrogen in leaf litter (in 2001) declines with increased density of *Alouatta seniculus* (r^2 = 0.23, $P < 0.05$).

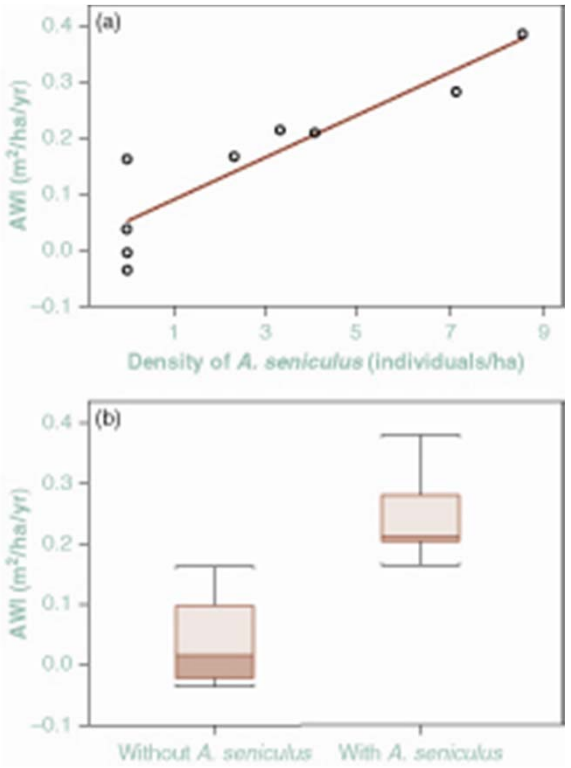

FIGURE 10–21

(a) The annual woody increment (AWI) of trees on the study islands increases with increased herbivore (*Alouatta seniculus*) density (r^2 = 0.82, P = 0.001). (b) AWI is, on average, 6.1 times greater on islands with *A. seniculus* than on islands without *A. seniculus* (*t* test, $P < 0.01$).